

1 **Is there an optimal ENSO pattern that increases U.S. tornado activity?**

2  
3  
4  
5  
6 Sang-Ki Lee<sup>1,2</sup>, David Enfield<sup>1,2</sup>, Hailong Liu<sup>1,2</sup>, Chunzai Wang<sup>2</sup>, Robert Atlas<sup>2</sup>, and Brian  
7 Mapes<sup>3</sup>

8 <sup>1</sup>Cooperative Institute for Marine and Atmospheric Studies, University of Miami, Miami,  
9 Florida, USA

10 <sup>2</sup>Atlantic Oceanographic and Meteorological Laboratory, NOAA, Miami Florida, USA  
11 USA

12 <sup>3</sup>Rosenstiel School of Marine and Atmospheric Science, University of Miami, Miami, Florida,  
13 USA

14  
15  
16 To be Submitted to Geophysical Research Letters

17 June 2011

18  
19  
20  
21  
22 Corresponding author address: Dr. Sang-Ki Lee, NOAA/AOML, 4301 Rickenbacker Causeway,  
23 Miami, FL 33149, USA. E-mail: [Sang-Ki.Lee@noaa.gov](mailto:Sang-Ki.Lee@noaa.gov).

1 **Abstract**

2 Observations and modeling experiments are used to show that a positive phase of Trans-  
3 Niño, characterized by cooling in the central tropical Pacific and warming in the eastern tropical  
4 Pacific, is linked to an increased number of intense U.S. tornadoes in spring. The warming in the  
5 eastern tropical Pacific increases convection locally, but also contributes to suppressing  
6 convection in the central tropical Pacific. This in turn works constructively with cooling in the  
7 central tropical Pacific to force a strong and persistent negative phase Pacific – North American  
8 teleconnection pattern. The anomalous winds that are associated with this teleconnection pattern  
9 bring more cold and dry upper-level air from the high-latitudes and more warm and moist lower-  
10 level air from the Gulf of Mexico converging into the central U.S., and thus provide favorable  
11 condition for increased U.S. tornado activity. Both observations and model experiments suggest  
12 that a positive phase of Trans-Niño that persisted in April and May of 2011 contributed to the  
13 series of extreme tornado outbreaks that occurred during the same period.

14  
15  
16  
17  
18  
19  
20  
21  
22  
23

1 **1. Introduction**

2 In April and May of 2011, a record breaking 1,243 tornadoes were reported in the United  
3 States. This resulted in 517 tornado related fatalities, making 2011 one of the deadliest tornado  
4 years in U.S. history [<http://www.spc.noaa.gov/climo/torn/fataltorn.html>]. Questions were raised  
5 almost immediately as to whether the series of extreme tornado outbreaks in 2011 could be  
6 linked to long-term climate changes. The severe weather database (SWD) from the National  
7 Oceanic and Atmospheric Administration indicates that the number of total U.S. tornadoes (i.e.,  
8 from F0 to F5 in Fujita-Pearson scale) during the most active tornado months of April and May  
9 (AM) has been steadily increasing since 1950 (Figure S1a). However, due to the improvements  
10 in tornado detection technology with time, one must be cautious in attributing this secular  
11 increase in the number of U.S. tornadoes to a specific long-term climate signal [Brooks and  
12 Doswell, 2001]. Since intense and long-lived tornadoes are much more likely to be detected and  
13 reported even before a national network of Doppler radar was build in the 1990s, the number of  
14 intense U.S. tornadoes (i.e., from F3 to F5 in Fujita-Pearson scale) in AM during 1950-2010 is  
15 obtained from the SWD (Figure S1b) and used, after detrending, as the primary diagnostic index  
16 in this study (Figure S1c).

17 In the central U.S. east of the Rocky Mountains, cold and dry upper-level air from the high  
18 latitudes often converges with warm and moist lower-level air coming from the Gulf of Mexico  
19 (GoM). Due to this so-called large-scale differential advection (i.e., two or more different air  
20 masses converging at different heights), a conditionally unstable atmosphere with high  
21 convective available potential energy is formed that causes frequent and intense thunderstorms.  
22 With the addition of a triggering mechanism, such as the horizontal spinning effect provided by  
23 the lower-level wind shear (i.e., wind speed increasing or wind direction changing with height),

1 these thunderstorms can spawn intense tornadoes. Consistently, the moisture transport from the  
2 GoM to the central U.S. is significantly correlated with the number of intense U.S. tornadoes in  
3 AM (see Table 1). See Rasmussen and Blanchard [1998], and Brooks et al. [2003] for various  
4 meteorological indices for estimating the occurrence of tornadoes.

5 The Pacific – North American (PNA) pattern in boreal winter and spring is linked to the  
6 large-scale differential advection in the central U.S. as discussed in earlier studies [e.g., Munoz  
7 and Enfield, 2011]. During a negative phase of the PNA, an anomalous cyclone is formed over  
8 North America that bring cold and dry upper-level air from the high latitudes to the central U.S.,  
9 and an anticyclone is formed over the southeastern seaboard that increases the southwesterly  
10 wind from the GoM to the central U.S., thus enhancing the Gulf-to-U.S. moisture transport.  
11 Although the PNA is a naturally occurring atmospheric phenomenon driven by the intrinsic  
12 variability of the atmosphere, a La Niña in the tropical Pacific can project onto a negative phase  
13 PNA pattern [e.g., Lau 1981; Wallace and Gutzler 1981; Straus and Shukla 2002]. In addition,  
14 since the Gulf-to-U.S. moisture transport can be enhanced with a warmer GoM, the sea surface  
15 temperature (SST) anomaly in the GoM can also affect U.S. tornado activity. During the decay  
16 phase of La Niña in spring, the GoM is typically warmer than usual [e.g., Alexander and Scott  
17 2002]. Therefore, the Gulf-to-U.S. moisture transport can be increased during the decay phase of  
18 La Niña in spring due to the increased SSTs in the GoM and the strengthening of the  
19 southwesterly wind from the GoM to U.S. Nevertheless, none of these (i.e., PNA, GoM SST, and  
20 La Nina) are significantly correlated with the number of intense tornadoes in AM (see Table 1)  
21 as demonstrated in earlier studies [e.g., Cook and Schaefer, 2008]. Currently, seasonal forecast  
22 skill for intense U.S. tornado outbreaks, such as occurred in 2011, has not been demonstrated.

1        Among the long-term climate patterns considered in Table 1, only the Trans-Niño (TNI) is  
2 significantly correlated ( $r = 0.33$ ) with the number of intense U.S. tornadoes in AM. TNI, which  
3 is defined as the difference in normalized SST anomalies between the Niño-1+2 ( $10^{\circ}\text{S} - 0^{\circ}$ ;  
4  $90^{\circ}\text{W} - 80^{\circ}\text{W}$ ) and Niño-4 ( $5^{\circ}\text{N} - 5^{\circ}\text{S}$ ;  $160^{\circ}\text{E} - 150^{\circ}\text{W}$ ) regions, represents the evolution of the  
5 El Niño-Southern Oscillation (ENSO) in the months leading up to the event and the subsequent  
6 evolution with opposite sign after the event [Trenberth and Stepaniak, 2001]. Given that AM is  
7 typically characterized with the development or decay phase of ENSO events, it is more likely  
8 that the tropical Pacific SST anomalies in AM are better represented by TNI index than the  
9 conventional ENSO indices such as Niño-3.4 ( $5^{\circ}\text{N} - 5^{\circ}\text{S}$ ;  $170^{\circ}\text{W} - 120^{\circ}\text{W}$ ) or Niño-3 ( $5^{\circ}\text{N} - 5^{\circ}\text{S}$ ;  
10  $150^{\circ}\text{W} - 90^{\circ}\text{W}$ ). Nevertheless, it is not at all clear why the number of intense U.S. tornadoes in  
11 AM is significantly correlated with the TNI index, but not with other ENSO indices. This is the  
12 central question that we explore in the following sections by using both observations and an  
13 atmospheric general circulation model (AGCM).

14

## 15 **2. Observations**

16        To better understand the potential link between TNI and U.S. tornado activity, we ranked the  
17 years from 1950 to 2010 (61 years in total) based on the number of intense U.S. tornadoes in  
18 AM. The top ten years are characterized by increased Gulf-to-U.S. moisture transport in the  
19 lower-level (Figure 1a) and an upper-level cyclone over North America that advects cold and dry  
20 air to the central U.S. (Figure 1c), whereas the bottom ten years are associated with decreased  
21 Gulf-to-U.S. moisture transport (Figure 1b) and an upper-level anticyclone over North America  
22 (Figure 1d). This is consistent with the notion that springtime U.S. tornado activity is modulated  
23 by the large-scale differential advection in the central U.S.

1 As shown in Table S1, among the top ten years, seven years including the top three are  
2 identified with a positive phase (i.e., above  $\frac{1}{4}$  quantile) TNI index (i.e., normalized SST  
3 anomalies are larger in the Niño-1+2 than in Niño-4 region). Five out of those seven years are  
4 characterized by a La Niña transitioning to a different phase or persisting beyond AM (1957,  
5 1965, 1974, 1999, and 2008) and the other two with an El Niño transitioning to either a La Nina  
6 or neutral phase (1983 and 1998). Figure 2a shows the composite SSTs for those five positive  
7 phase TNI years transitioning from a La Niña.

8 On the other hand, among the bottom ten years, only one year is identified with a positive  
9 phase TNI, and the other nine years are with a neutral phase (i.e., between  $\frac{1}{4}$  and  $\frac{3}{4}$  quantile)  
10 TNI (see Table S2), suggesting that a negative phase TNI does not either decrease or increase the  
11 number of intense U.S. tornadoes in AM. Interestingly, four years among the bottom ten years  
12 are identified with a La Niña transitioning to a different phase or persisting beyond AM (1950,  
13 1951, 1955 and 2001), and four are with an El Niño transitioning to a different phase or  
14 persisting beyond AM (1958, 1987, 1988 and 1992). As shown in Figure 2b, the SST anomaly  
15 pattern for the four years with a La Niña transitioning is that of a typical La Niña with the SST  
16 anomalies in the Niño-4 and Niño-1+2 being both strongly negative (i.e., neutral phase TNI).  
17 Similarly, as shown in Figure 2c, the SST anomaly pattern for the four years with an El Niño  
18 transitioning is that of a typical El Niño with the SST anomalies in the Niño-4 and Niño-1+2  
19 being both strongly positive (i.e., neutral phase TNI).

20 In summary, observations indicate that a positive phase TNI (i.e., normalized SST anomalies  
21 are larger in Niño-1+2 than in Niño-4 region) is linked to increased number of intense U.S.  
22 tornadoes in AM, whereas both the La Niñas and El Niños with a neutral phase TNI (i.e., the

1 SST anomalies in the Niño-1+2 region are as strong and the same sign as the SST anomalies in  
2 the Niño-4) are linked to a decreased number of intense U.S. tornadoes in AM.

3

### 4 **3. Model Experiments**

5 To explore the potential link between the three tropical Pacific SST patterns (see Figure 2),  
6 identified in the previous section, and the number of intense U.S. tornadoes in AM, a series of  
7 AGCM experiments are performed by using version 3.1 of the NCAR community atmospheric  
8 model coupled to a slab mixed layer ocean model (CAM3). The model is a global spectral model  
9 with a triangular spectral truncation of the spherical harmonics at zonal wave number 42 (T42).  
10 It is vertically divided into 26 hybrid sigma-pressure layers. Model experiments are performed  
11 by prescribing various composite evolutions of SSTs in the tropical Pacific region (15°S–15°N;  
12 120°E-coast of the Americas) while predicting the SSTs outside the tropical Pacific using the  
13 slab ocean model. To prevent discontinuity of SST around the edges of the forcing region, the  
14 model SSTs of three grid points centered at the boundary are determined by combining the  
15 simulated and prescribed SST. Each ensemble consists of ten model integrations that are  
16 initialized with slightly different conditions to represent internal atmospheric variability. The  
17 same methodology was previously used in Lee et al. [2008] for studying ENSO teleconnection to  
18 the tropical North Atlantic region.

19 Four sets of ensemble runs are performed (see Table S3). In the first experiment  
20 (EXP\_CLM), the SSTs in the tropical Pacific region are prescribed with climatological SSTs. In  
21 the second experiment (EXP\_TNI), the composite SSTs of the positive phase TNI years  
22 identified among the ten most active U.S. tornado years are prescribed in the tropical Pacific  
23 region. Note that only the five TNI years transitioning from a La Niña (1957, 1965, 1974, 1999,

1 and 2008) are considered here because the other two negative TNI years are transitioning from  
2 an El Niño (1983 and 1998) and thus tend to cancel the tropical SST anomalies of the other five.  
3 In the next two experiments, the SSTs in the tropical Pacific region are prescribed with the  
4 composite SSTs of the four years with a La Niña transitioning (1950, 1951, 1955 and 2001) and  
5 the four years with an El Niño transitioning (1958, 1987, 1988 and 1992) in EXP\_LAN and in  
6 EXP\_ELN, respectively identified among the ten least active U.S. tornado years.

7

#### 8 **4. Model Results**

9 Figure 3 and S2 show the simulated moisture transport, and geopotential height and wind at  
10 500 hPa in AM obtained from the three model experiments. In EXP\_TNI (Figure 3), the Gulf-to-  
11 U.S. moisture transport is greatly increased and an upper-level cyclone is formed over North  
12 America that brings more cold and dry air to the central U.S., all indicating enhanced large-scale  
13 differential advection in the central U.S. In EXP\_LAN and EXP\_ELN (Figure S2), on the other  
14 hand, the Gulf-to-U.S. moisture transport is not either increased or decreased. A relatively weak  
15 upper-level cyclone is formed in EXP\_LAN, but it is positioned over the eastern seaboard. In  
16 EXP\_ELN, a weak upper-level anticyclone is formed and also positioned over the eastern  
17 seaboard.

18 Therefore, these model results fully support the hypothesis that a positive phase TNI with  
19 cooling in the central tropical Pacific (CP) and warming in the eastern tropical Pacific (EP)  
20 enhances the large-scale differential advection in the central U.S. advecting cold and dry upper-  
21 level air from the high-latitudes and warm and moist lower-level from the GoM, and thus  
22 increasing U.S. tornado activity in the spring. However, the model results do not show any  
23 increase or decrease in the large-scale differential advection in the central U.S. by La Niña and



1 El Niño conditions as long as the SST anomalies in EP are as strong and the same sign as the  
2 SST anomalies in CP.

3

#### 4 **5. CP- versus EP-forced Teleconnection**

5 The model results strongly suggest that cooling in CP and warming in EP may have a  
6 constructive influence on the teleconnection pattern that strengthens the large-scale differential  
7 advection over the central U.S. One possibility is that the Rossby wave train forced by warming  
8 in EP may have the same spatial structure as that forced by cooling in CP but shifted eastward  
9 with the sign reversed. The two linearly independent Rossby wave trains may be superimposed  
10 to each other in such a way as to enhance the large-scale differential advection over the central  
11 U.S. Such a mechanism is partially supported by the simple two-level dry atmosphere model  
12 [Lee et al. 2009] forced with cooling in CP and warming EP (not shown).

13 To better understand how the real atmosphere with moist diabatic processes responds to CP  
14 cooling and EP warming, two sets of additional model experiments (EXP\_CPC and EXP\_EPW)  
15 are performed (see Table S3). These two experiments are basically identical to EXP\_TNI except  
16 that the composite SSTs of the positive phase TNI years are prescribed only in the western and  
17 central tropical Pacific region (15°S–15°N; 120°E - 110°W) for EXP\_CPC and only in the  
18 eastern tropical Pacific region (15°S–15°N; 110°W-coast of the Americas) for EXP\_EPW.

19 Figure 4 show the simulated moisture transport, and geopotential height and wind at 500 hPa,  
20 in AM obtained from the two additional model experiments. In EXP\_CPC, the teleconnection  
21 pattern emanating from the tropical Pacific consists of an anticyclone over the Aleutian Low in  
22 the North Pacific, a cyclone over North America, and an anticyclone over the southeastern U.S.  
23 and central Americas, consistent with a typical negative phase PNA pattern (Figure 4c). As

1 expected from the anomalous anticyclone over the southeastern U.S. and central Americas, the  
2 Gulf-to-U.S. moisture transport is increased in EXP\_CPC (Figure 4b).

3 Surprisingly, the Rossby wave train forced by a warming in EP (EXP\_EPW) is very similar  
4 to that in EXP\_CPC (Figure 4f). Consistently, the Gulf-to-U.S. moisture transport is also  
5 increased in EXP\_EPW as in EXP\_CPC and EXP\_TNI (Figure 4e). The teleconnection pattern  
6 in EXP\_EPW is not either shifted eastward or its sign reversed from that in EXP\_CPC.  
7 Obviously, a question arises as to why the teleconnection pattern forced by warming in EP is  
8 virtually the same as that forced by cooling in CP. It appears that the Rossby wave train in  
9 EXP\_EPW is not directly forced from EP. As shown in Figure S3c, in EXP\_EPW, convection is  
10 increased locally in EP, but it is decreased in CP as in EXP\_CPC. This suggests that increased  
11 convection in EP associated with the increased local SSTs suppresses convection in CP that in  
12 turn forces a negative phase PNA-like pattern. These model results confirm that cooling in CP  
13 and warming in EP do have constructive influence on the teleconnection pattern that strengthens  
14 the large-scale differential advection over the central U.S. The model results also suggest that  
15 cooling in CP with neutral SST anomalies in EP or warming in EP with neutral SST anomalies in  
16 CP can strengthen the large-scale differential advection over the central U.S.

17 An apparently important question is why warming in EP does not directly excite a Rossby  
18 wave train to the high-latitudes. As shown in earlier theoretical studies, the vertical background  
19 wind shear is a critical factor that determines the amplitude of teleconnection to high-latitudes  
20 [e.g., Lee et al. 2008]. Figure S4 clearly shows that, in both observations and EXP\_CLM, the  
21 background vertical wind shear between 200 and 850 hPa in AM is largest in the central tropical  
22 North Pacific and smallest in EP and the western tropical Pacific (WP), clearly explaining why

1 the Rossby wave train in EXP\_EPW is not directly forced in EP (Figure 4f). See Lee et al.  
2 [2008] for more discussions on this issue.

3

#### 4 **6. Effect of Intrinsic Variability**

5 The conclusion so far is that a positive phase TNI with cooling in CP and warming in EP can  
6 increase U.S. tornado activity in spring because the CP cooling and EP warming have  
7 constructive influence on the teleconnection pattern that strengthens the large-scale differential  
8 advection over the central U.S. However, the correlation between TNI and the number of intense  
9 U.S. tornadoes in AM is only 0.33 indicating that TNI can explain only about 10% of the total  
10 variance. This suggests that intrinsic variability in the atmosphere may overwhelm a negative  
11 phase TNI-forced teleconnection pattern over North America as discussed in earlier studies for  
12 El Niño teleconnection patterns in the Pacific–North American region [e.g., Hoerling and  
13 Kumar, 1997]. In order to better illustrate this point, we select neutral TNI years during 1950-  
14 2010 and divide them into one group with an increased Gulf-to-U.S. moisture transport in AM  
15 and the other group with a decreased Gulf-to-U.S. moisture transport. Figure S5b shows the  
16 difference in moisture transport between these two groups. Similarly, we divide ten ensemble  
17 experiments for EXP\_CLM into two groups, one with an increased Gulf-to-U.S. moisture  
18 transport in AM and the other group with a decreased Gulf-to-U.S. moisture transport. Figure  
19 S5c shows the difference in moisture transport between these two groups.

20 As expected, the typical amplitude of Gulf-to-U.S. moisture transport induced by intrinsic  
21 variability in the atmosphere such as the PNA during neutral phase TNI years is larger than the  
22 anomalous Gulf-to-U.S. moisture transport for positive phase TNI years (Figure S5a). Similarly,  
23 internal variability in EXP\_CLM can generate anomalous Gulf-to-U.S. moisture transport with

1 comparable amplitude to that simulated in EXP\_TNI. Therefore, we can conclude that the  
2 strengthening of the large-scale differential advection over the central U.S. during a positive  
3 phase of TNI can be greatly reduced or enhanced by internal variability in the atmosphere. In  
4 other words, although seven of the ten most active tornado years during 1950-2010 including the  
5 top three years are characterized with a strongly positive phase TNI (see Table S1), the  
6 associated predictability of U.S. tornado activity, which can be defined as a ratio of the climate  
7 signal (TNI in this case) relative to the climate noise, is low.

8

## 9 **7. U.S. Tornado Outbreaks in 2011**

10 As shown in Figure S6a, a positive phase of TNI prevailed during AM of 2011 with cooling  
11 in CP and warming EP. An important question is whether the series of extreme U.S. tornado  
12 outbreaks during AM of 2011 can be attributed to this positive TNI. During AM of 2011, an  
13 upper-level anticyclone is formed over North America (Figure S6c), and the Gulf-to-US  
14 moisture is greatly increased (Figure S6b), both indicating the coherent teleconnection response  
15 to a positive phase TNI. To confirm this, a set of model experiments (EXP\_011) is performed by  
16 prescribing the 2010-2011 SSTs in the tropical Pacific region while predicting the SSTs outside  
17 the tropical Pacific using the slab ocean model (see Table S3). As summarized in Figure S7, the  
18 model results are consistent with the observations (Figure S6). Further model experiments (see  
19 Table S3) also show that the warming in WP, which is a distinctive feature in the TNI event in  
20 2011, indirectly suppresses convection in CP, and thus works constructively with the cooling in  
21 CP to force a strong and persistent negative phase PNA-like pattern (Figure S8 and S9).  
22 However, due to the low signal-to-noise ratio in the TNI-induced teleconnection response in the  
23 central U.S., it is only safe to say that the positive phase of TNI in AM of 2011 *contributed* to the

1 increased number of intense U.S. tornadoes during the same period by enhancing the differential  
2 advection in the central U.S.

3

#### 4 **8. Discussion**

5 The record-breaking U.S. tornado outbreak in the spring of 2011 prompts the need to identify  
6 and understand long-term climate signals that provide seasonal predictability for intense tornado  
7 outbreaks. Here, we use both observations and modeling experiments to demonstrate that a  
8 positive phase of TNI, characterized by cooling in CP and warming in EP, is one such climate  
9 pattern that can strengthen the large-scale differential advection in the central U.S. and thus  
10 increase U.S. tornado activity. Both observations and model experiments suggest that a positive  
11 phase of Trans-Niño that persisted in AM of 2011 contributed to the series of extreme tornado  
12 outbreaks that occurred during the same period. However, although seven of the ten most active  
13 tornado years during 1950 – 2010 including the top three are characterized with a strongly  
14 positive phase of TNI, TNI explains only 10% of the total variance in the number of intense U.S.  
15 tornadoes in AM. Therefore, further study is needed to refine the predictive skill provided by  
16 TNI and to explore other long-term climate signals that can provide additional predictability in  
17 seasonal and longer time scales. A potentially important long-term signal not explicitly explored  
18 in this study is what appears to be a shift in the number of intense U.S. tornadoes in AM around  
19 1980 (Figure S1b). Although it is unclear whether this shift is real or a bias in the SWD, it is in  
20 line with the shift in the PDO phase that occurred around the same time. It is possible that the in-  
21 phase combination of ENSO and Pacific Decadal Oscillation (PDO) leads to stronger and more  
22 persistent PNA-like teleconnection pattern [e.g., Yu and Zwiers, 2007].

23

1 **Acknowledgments.** This study was motivated and benefited from interactions with scientists at  
2 NOAA ESRL, GFDL, CPC, and NCDC. In particular, we wish to thank Tom Karl for posing the  
3 question that motivated this study. This work was supported by grants from the National Oceanic  
4 and Atmospheric Administration’s Climate Program Office and by grants from the National  
5 Science Foundation.

6

7

### References

8 Alexander, M., and J. Scott (2002), The influence of ENSO on air-sea interaction in the Atlantic.  
9 *Geophys. Res. Lett.*, **29**, 1701. doi:10.1029/2001GL014347.

10 Brooks, H. E., C. A. Doswell III (2001), Some aspects of the international climatology of  
11 tornadoes by damage classification, *Atmos. Res.*, **56**, 191– 201.

12 Brooks, H. E., J. W. Lee, and J. P. Cravenc (2003), The spatial distribution of severe  
13 thunderstorm and tornado environments from global reanalysis data, *Atmos. Res.*, **67-68**, 73-  
14 94.

15 Cook, A. R., and J. T. Schaefer (2008), The relation of El Niño–Southern Oscillation (ENSO) to  
16 winter tornado outbreaks, *Mon. Wea. Rev.*, **136**, 3121–3137.

17 Hoerling, M. P., and A. Kumar (1997), Why do North American climate anomalies differ from  
18 one El Niño event to another?, *Geophys. Res. Lett.*, **24**, 1059-1062.

19 Lau, N.-C., and M. J. Nath (2001), Impact of ENSO on SST variability in the North Pacific and  
20 North Atlantic: Seasonal dependence and role of extratropical air-sea coupling, *J. Clim.*, **14**,  
21 2846–2866.

22 Lee, S.-K., D. B. Enfield and C. Wang (2008), Why do some El Ninos have no impact on  
23 tropical North Atlantic SST? *Geophys. Res. Lett.*, **35**, L16705, doi:10.1029/2008GL034734.

1 Lee, S.-K., C. Wang and B. E. Mapes (2009), A simple atmospheric model of the local and  
2 teleconnection responses to tropical heating anomalies. *J. Clim.*, **22**, 272-284.

3 Munoz, E., and D. Enfield (2010), The boreal spring variability of the Intra-Americas low-level  
4 jet and its relation with precipitation and tornadoes in the eastern United States, *Clim. Dyn.*  
5 **36**, 247–259.

6 Rasmussen, E. N., D. O. Blanchard (1998), A baseline climatology of sounding-derived  
7 supercell and tornado forecast parameters. *Weather Forecast.* **13**, 1148–1164.

8 Straus, D. M., and J. Shukla (2002), Does ENSO force the PNA?, *J. Clim.*, **15**, 2340–2358.

9 Trenberth, K. E., and D. P. Stepaniak (2001), Indices of El Niño evolution, *J. Clim.*, 14, 1697–  
10 1701.

11 Wallace, J. M., and D. S. Gutzler (1981), Teleconnections in the geopotential height field during  
12 the Northern Hemisphere Winter, *Mon. Wea. Rev.*, **109**, 784-812.

13 Yu, B., and F. W. Zwiers (2007), The impact of combined ENSO and PDO on the PNA climate:  
14 a 1,000-year climate modeling study, *Clim. Dyn.*, **29**, 837-851.

15  
16  
17  
18  
19  
20  
21  
22  
23

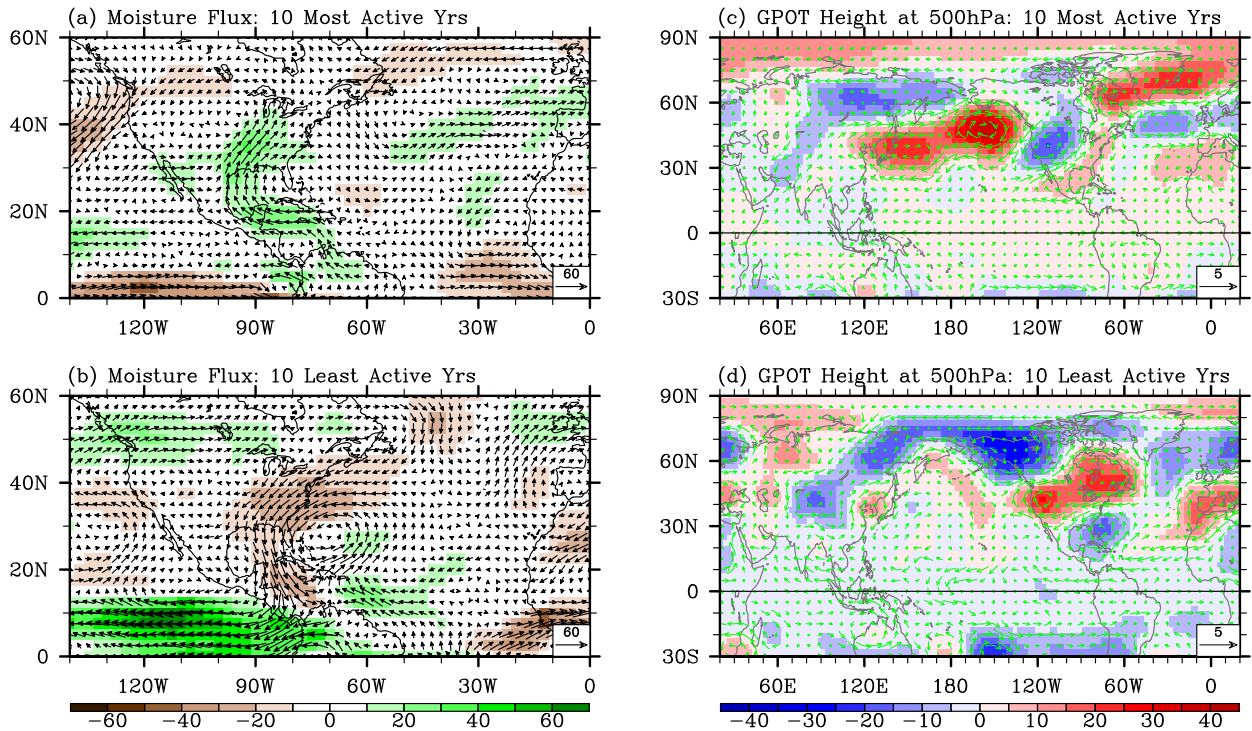
1 **Table 1.** Correlation coefficients of various long-term climate patterns with the number of  
2 intense (F3 - F5) tornados in April and May (AM) during 1950-2010. All indices including the  
3 tornado index are detrended. The SWD, ERSST3, and NCEP-NCAR reanalysis are used to  
4 obtain the long-term climate indices used in this table. Any correlation value with above the 95%  
5 significance is in bold<sup>a</sup>

Index	DJF	FMA	AM
Gulf-to-U.S. moisture transport	0.08	0.20	<b>0.40</b>
GoM SST	0.15	0.21	0.20
Niño-4	-0.22	-0.20	-0.19
Niño-3.4	-0.13	-0.13	-0.11
Niño-1+2	0.02	0.11	0.15
TNI	<b>0.28</b>	<b>0.29</b>	<b>0.33</b>
PNA	-0.05	-0.10	-0.20
PDO	-0.12	-0.10	-0.14
NAO	-0.01	-0.10	-0.18

6 <sup>a</sup>The Gulf-to-U.S. meridional moisture transport is obtained by averaging the vertically  
7 integrated moisture transport in the region of 25°N - 35°N and 100°W - 90°W. The North  
8 Atlantic Oscillation (NAO) index is defined as the first leading mode of Rotated Empirical  
9 Orthogonal Function (REOF) analysis of monthly mean 500 hPa. The Pacific Decadal  
10 Oscillation (PDO) is the leading principal component of monthly SST anomalies in the North  
11 Pacific Ocean north of 20°N. The Pacific - North American (PNA) pattern is defined as the  
12 second leading mode of REOF analysis of monthly mean 500 hPa.



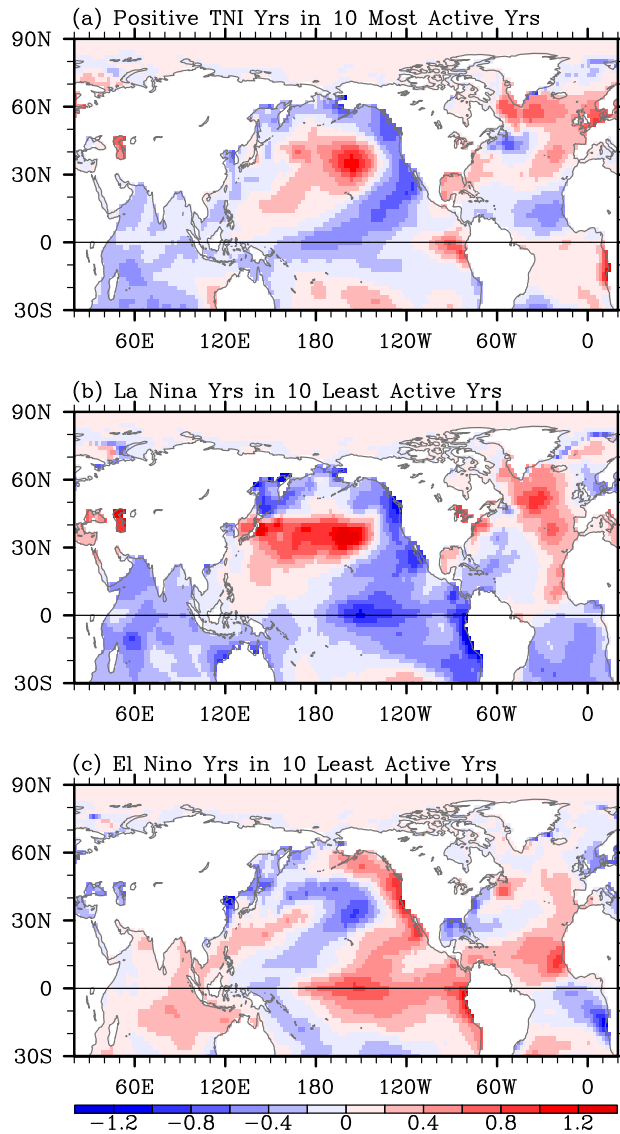
NCEP-NCAR Reanalysis: Moisture Flux and GPOT Height at 500hPa (APR-MAY)



1  
2 **Figure 1.** Anomalous moisture transport for (a) the ten most active U.S. tornado years and (b)  
3 the ten least active U.S. tornado years in AM during 1950-2010 obtained from NCEP-NCAR  
4 reanalysis. Anomalous geopotential height and wind at 500 hPa for (c) the ten most active U.S.  
5 tornado years and (d) the ten least active U.S. tornado years in AM during 1950-2010 obtained  
6 from NCEP-NCAR reanalysis. The unit is  $\text{kg m}^{-1}\text{sec}^{-1}$  for moisture transport, m for geopotential  
7 height, and  $\text{m s}^{-1}$  for wind.

8  
9  
10  
11  
12  
13

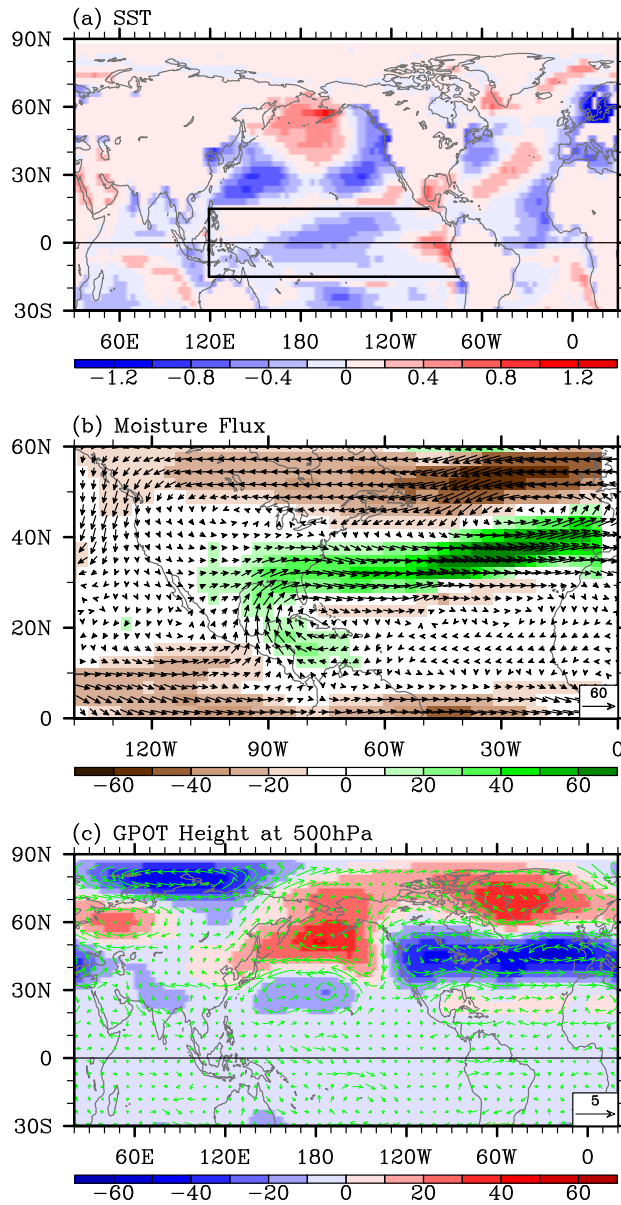
ERSST3: SST Anomalies (APR–MAY)



1  
2  
3  
4  
5  
6  
7  
8

**Figure 2.** Composite SST anomalies in AM, obtained from ERSST3, for (a) the five positive TNI years transitioning from a La Niña identified among the 10 most active U.S. tornado years in AM during 1950-2010, and for (b) the four years with a La Niña transitioning and (c) the four years with an El Niño transitioning identified among the 10 least active U.S. tornado years in AM during 1950-2010.

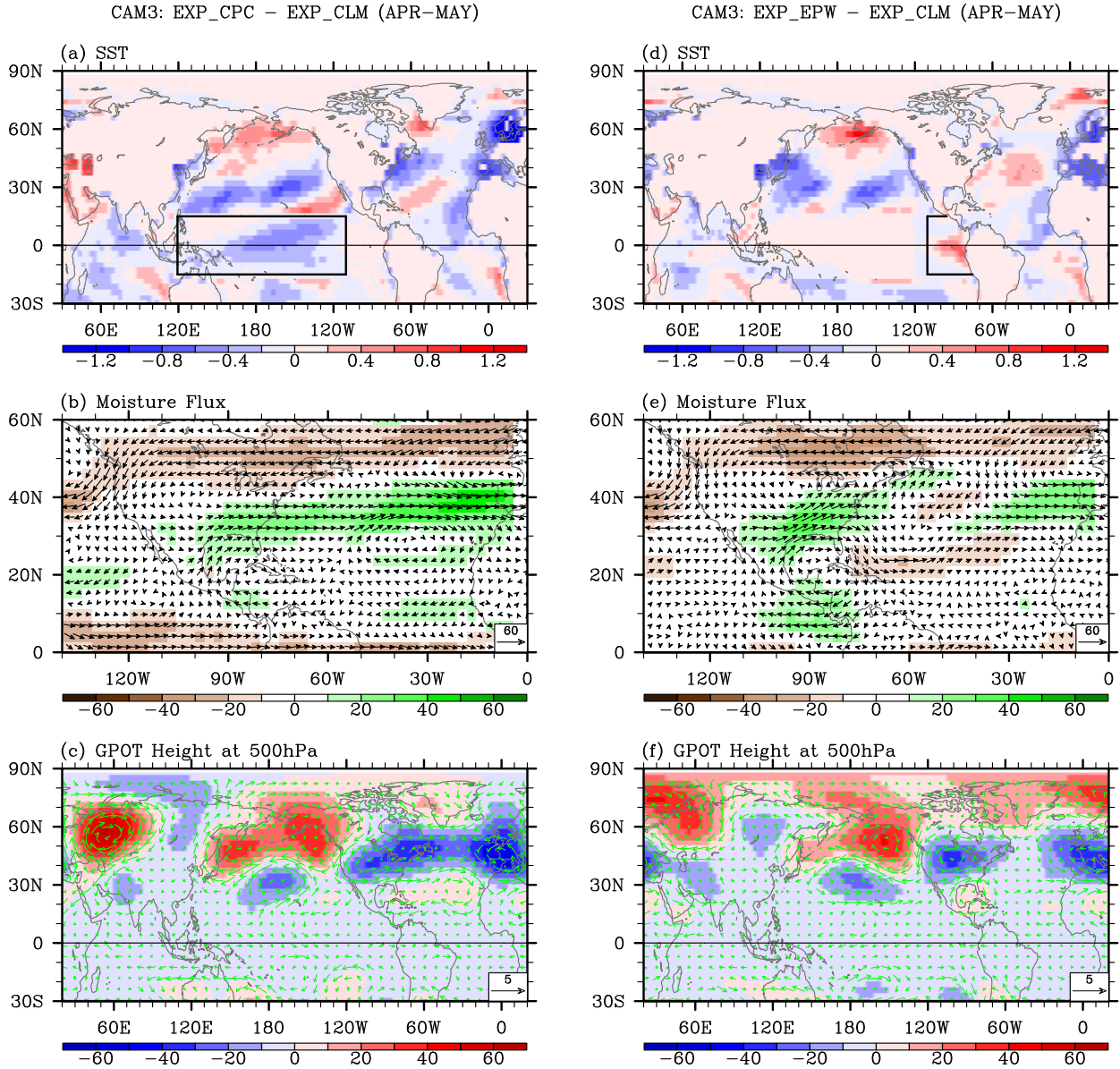
CAM3: EXP\_TNI - EXP\_CLM (APR-MAY)



1  
2 **Figure 3.** Simulated (a) SST, (b) moisture transport, and (c) geopotential height and wind at 500  
3 hPa in AM obtained from EXP\_TNI - EXP\_CLM. The unit is °C for SST,  $\text{kg m}^{-1} \text{sec}^{-1}$  for  
4 moisture transport, m for geopotential height,  $\text{m s}^{-1}$  for wind. Thick black lines in (a) indicate the  
5 tropical Pacific region where the model SSTs are prescribed.

6

7



1  
 2 **Figure 4.** Simulated (a) SST, (b) moisture transport, and (c) geopotential height and wind at 500  
 3 hPa in AM obtained from EXP\_CPC - EXP\_CLM. Simulated (d) SST, (e) moisture transport,  
 4 and (f) geopotential height and wind at 500 hPa in AM obtained from EXP\_EPW - EXP\_CLM.  
 5 The unit is  $^{\circ}\text{C}$  for SST,  $\text{kg m}^{-1} \text{sec}^{-1}$  for moisture transport, m for geopotential height, and  $\text{m s}^{-1}$   
 6 for wind. Thick black lines in (a) and (d) indicate the regions where the model SSTs are  
 7 prescribed.

**Table S1.** The total of 61 years from 1950 to 2010 are ranked based on the detrended number of intense U.S. tornadoes in AM. The top ten most active U.S. tornado years are listed with ENSO phase in spring and TNI index in AM for each year. Strongly positive (above  $\frac{1}{4}$  quantile) and negative (below  $\frac{3}{4}$  quantile) TNI index values are in bold and italic, respectively.

Ranking	Year	ENSO phase in spring	TNI index (detrended)
1	1974	La Niña persists	<b>1.30 ( 1.48)</b>
2	1965	La Niña transitions to El Niño	<b>1.39 ( 1.54)</b>
3	1957	La Niña transitions to El Niño	<b>0.57 ( 0.69)</b>
4	1982	El Niño develops	<i>-1.11 (-0.89)</i>
5	1973	El Niño transitions to La Niña	-0.42 (-0.24)
6	1999	La Niña persists	<b>0.47 ( 0.75)</b>
7	1983	El Niño decays	<b>1.86 ( 2.08)</b>
8	2003	El Niño decays	<i>-1.24 (-0.94)</i>
9	2008	La Niña decays	<b>1.41 ( 1.73)</b>
10	1998	El Niño transitions to La Niña	<b>1.69 ( 1.97)</b>

**Table S2.** The total of 61 years from 1950 to 2010 are ranked based on the detrended number of intense U.S. tornadoes in AM. The bottom ten years are listed with ENSO phase in spring and TNI index in AM for each year. Strongly positive (above  $\frac{1}{4}$  quantile) and negative (below  $\frac{3}{4}$  quantile) TNI index values are in bold and italic, respectively.

Ranking	Year	ENSO phase in spring	TNI index (detrended)
52	1958	El Niño decays	-0.61 (-0.49)
53	1955	La Niña persists	-0.27 (-0.16)
54	2001	La Niña decays	0.21 ( 0.50)
55	1986	El Niño develops	-0.39 (-0.16)
56	1988	El Niño transitions to La Niña	-0.37 (-0.13)
57	1987	El Niño persists	0.10 ( 0.34)
58	1992	El Niño decays	0.21 ( 0.47)
59	1952	Neutral	-0.67 (-0.57)
60	1951	La Niña transitions to El Niño	-0.31 (-0.22)
61	1950	La Niña persists	<b>0.77 ( 0.86)</b>

**Table S3.** SSTs in the tropical Pacific region prescribed for each model experiment. All model experiments are performed for two years starting from January of previous year.

Experiments	Prescribed SSTs in the tropical Pacific region
EXP_CLM	Climatological SSTs are prescribed in the tropical Pacific region (15°S–15°N; 120°E-coast of the Americas).
EXP_TNI	Composite SSTs of the five positive phase TNI years transiting from a La Niña identified among the ten most active U.S. tornado years (1957, 1965, 1974, 1999, and 2008) are prescribed in the tropical Pacific region.
EXP_LAN	Composite SSTs of the four years with a La Niña transitioning (1950, 1951, 1955 and 2001) identified among the ten least active U.S. tornado years are prescribed in the tropical Pacific region.
EXP_ELN	Composite SSTs of the four years with an El Niño transitioning (1958, 1987, 1988 and 1992) identified among the ten least active U.S. tornado years are prescribed in the tropical Pacific region
EXP_CPC	Same as EXP_TNI except that the composite SSTs are prescribed only in the western and central tropical Pacific region (15°S–15°N; 120°E - 110°W).
EXP_EPW	Same as EXP_TNI except that the composite SSTs are prescribed only in the eastern tropical Pacific region (15°S–15°N; 110°W-coast of the Americas).
EXP_011	2010-2011 SSTs are prescribed in the tropical Pacific region.
EXP_WPW	Same as EXP_011 except that 2010-2011 SSTs are prescribed only in the western Pacific region (15°S–15°N; 120°E - 180°).

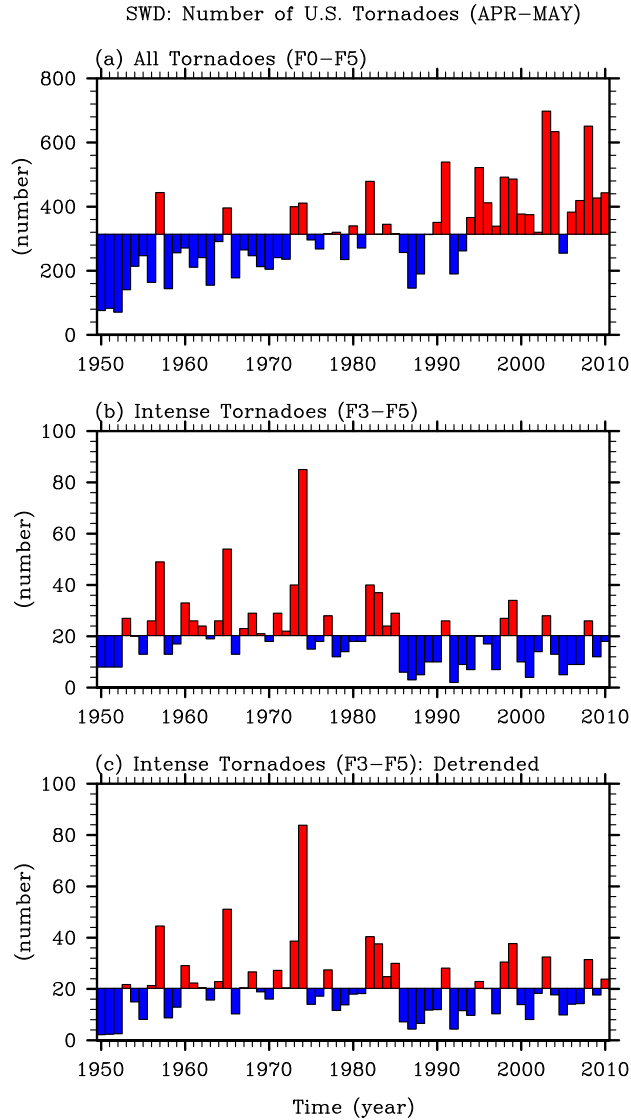


**Figure S1.** The number of (a) total (F0 – F5) and (b) intense (F3 – F5) US tornadoes for the most active tornado months of April and May (AM) during 1950-2010 obtained from SWD. The detrended number of intense U.S. tornadoes in AM, which is the primary diagnostic index used in this study, is shown in (c).



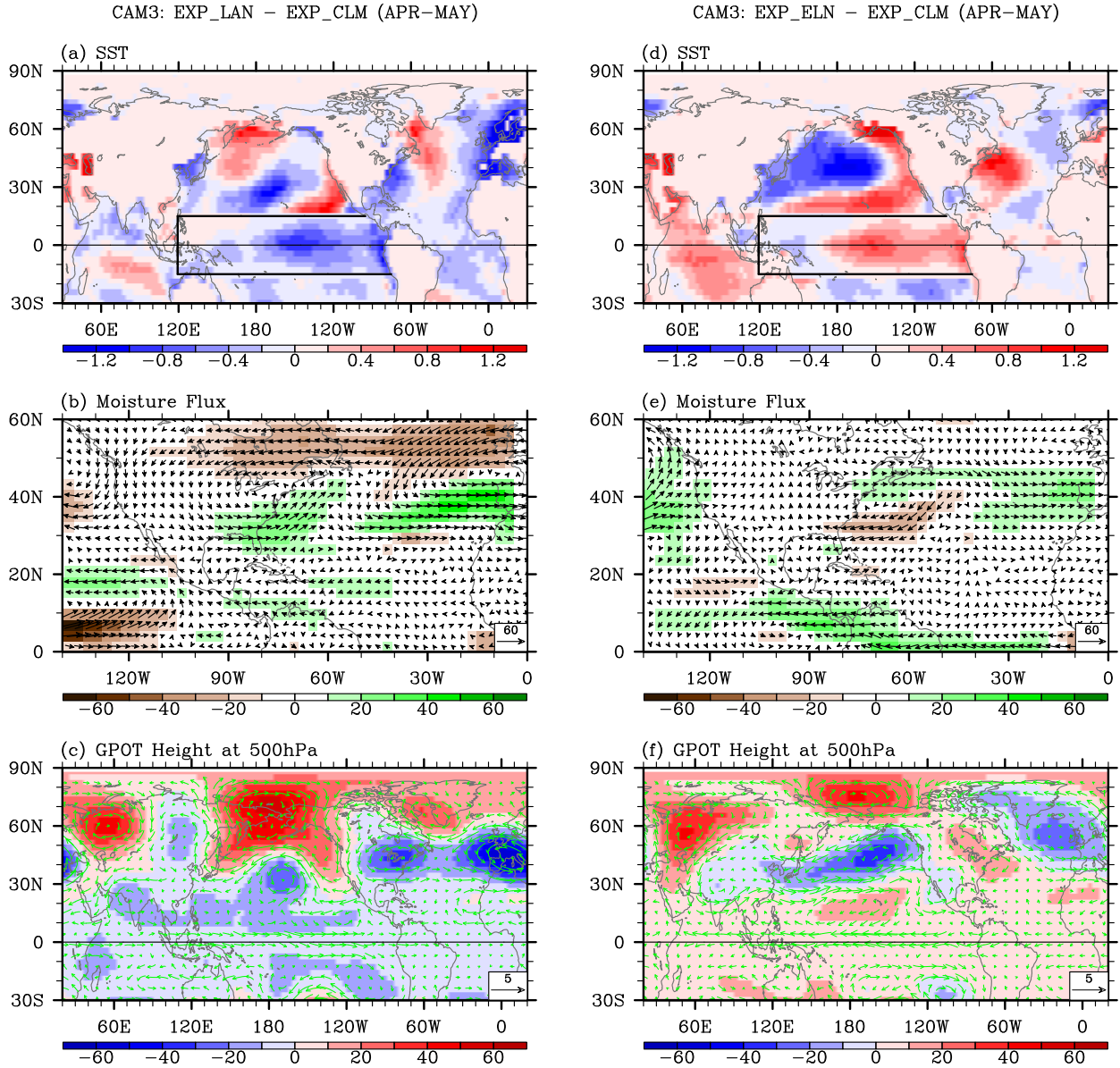


**Figure S2.** Simulated (a) SST, (b) moisture transport, and (c) geopotential height and wind at 500 hPa in AM obtained from EXP\_LAN – EXP\_CLM. Simulated (d) SST, (e) moisture transport, and (f) geopotential height and wind at 500 hPa in AM obtained from EXP\_ELN – EXP\_CLM. The unit is  $^{\circ}\text{C}$  for SST,  $\text{kg m}^{-1} \text{sec}^{-1}$  for moisture transport, m for geopotential height, and  $\text{m s}^{-1}$  for wind. Thick black lines in (a) and (d) indicate the tropical Pacific region where the model SSTs are prescribed.

CAM3: Convective Precipitation (APR-MAY)

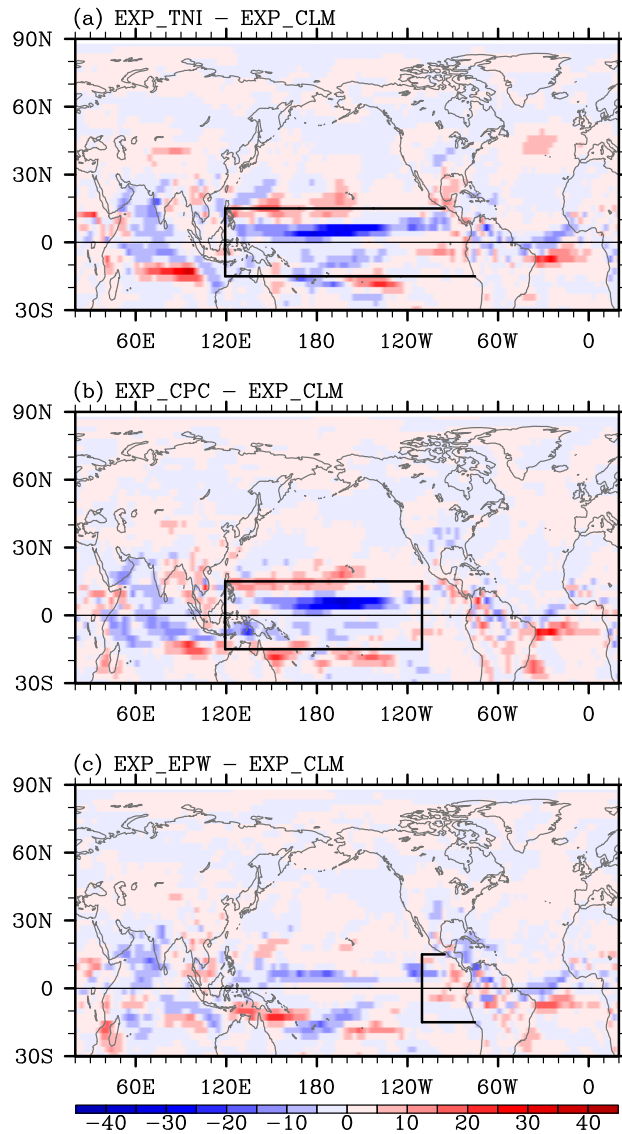


**Figure S3.** Simulated convective precipitation rate in AM obtained from (a) EXP\_TNI - EXP\_CLM, (b) EXP\_CPC - EXP\_CLM, and (c) EXP\_EPW - EXP\_CLM. The unit is mm day<sup>-1</sup>.

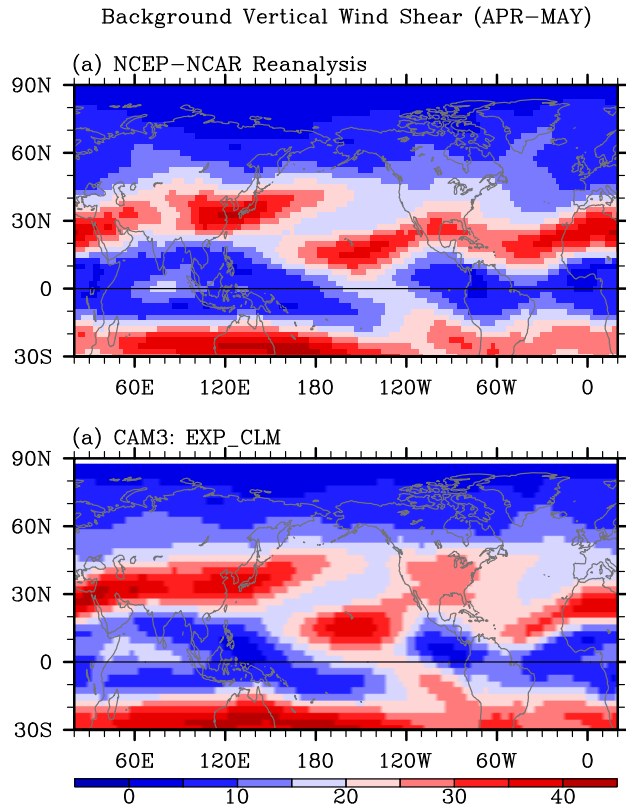


**Figure S4.** Background (climatological) vertical wind shear between 200 and 850 hPa in AM obtained from (a) NCEP-NCAR reanalysis, and (b) EXP\_CLM. The unit is  $\text{m sec}^{-1}$ .

Moisture Flux (APR–MAY)

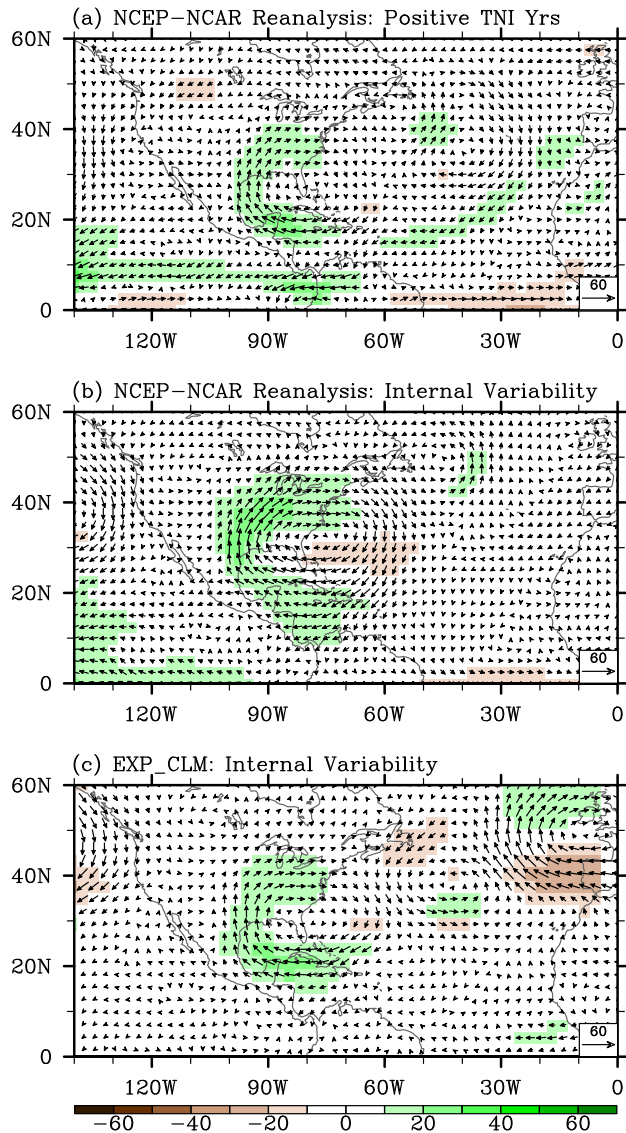


**Figure S5.** (a) Anomalous moisture transport in positive (above  $\frac{1}{4}$  quantile) TNI years during 1950–2010. Neutral TNI years during 1950–2010 are divided into one group with increased Gulf-to-US moisture transport in AM and the other group with decreased Gulf-to-US moisture transport. (b) The difference in moisture transport between these two groups from NCEP–NCAR reanalysis. Similarly, ten ensemble experiments for EXP\_CLM are divided into two groups, one with increased Gulf-to-US moisture transport in AM and the other group with decreased Gulf-to-US moisture transport. (c) The difference in moisture transport between these two groups from EXP\_CLM. The unit is  $\text{kg m}^{-1} \text{sec}^{-1}$ .

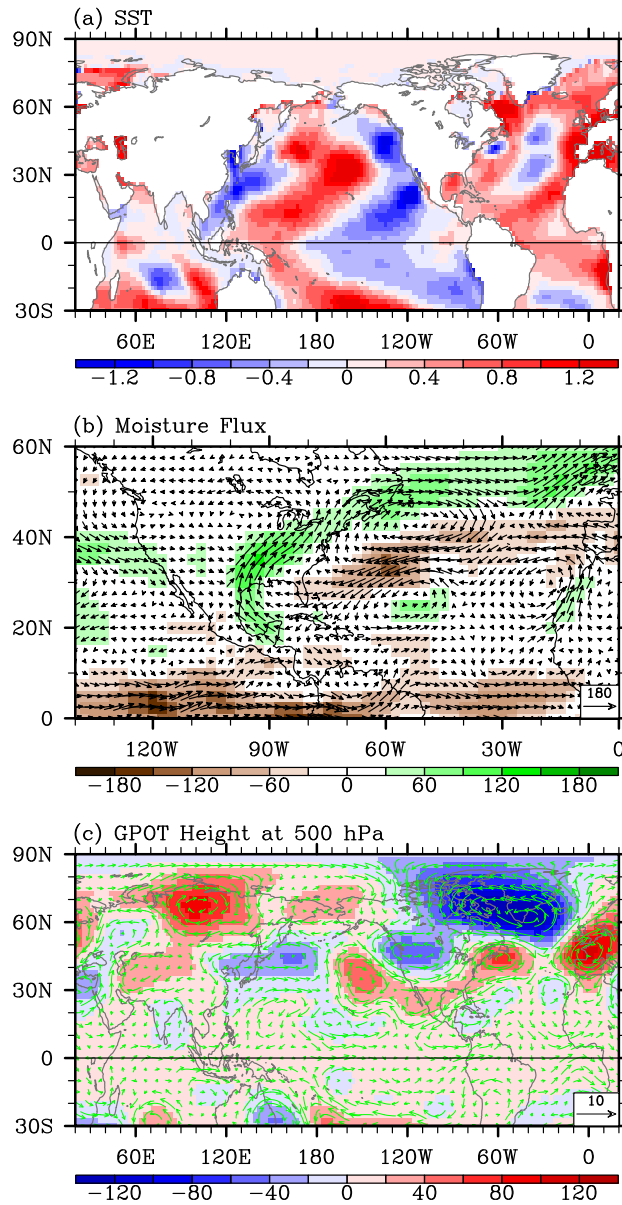


**Figure S6.** Anomalous (a) SST, (b) moisture transport, and (c) geopotential height and wind at 500 hPa in AM of 2011. The SST is obtained from ERSST3. The moisture transport, geopotential height, and wind are obtained from NCEP-NCAR reanalysis. The unit is °C for SST, kg m<sup>-1</sup> sec<sup>-1</sup> for moisture transport, m for geopotential height, and m s<sup>-1</sup> for wind.

CAM3: EXP\_011 - EXP\_CLM (APR-MAY)

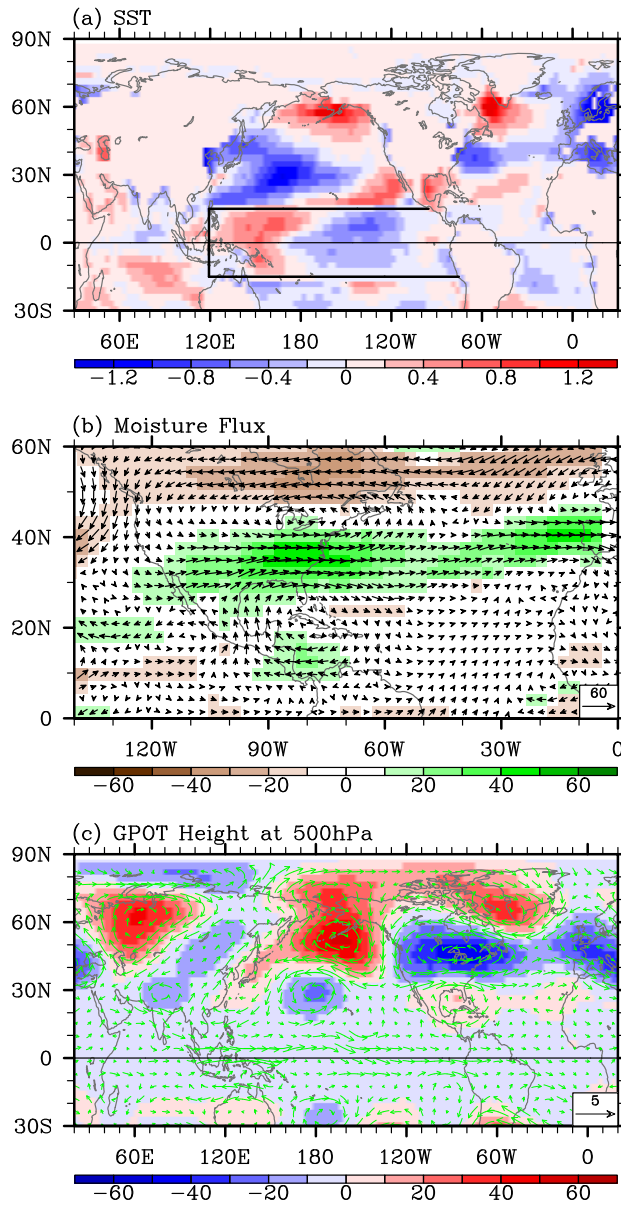


**Figure S7.** Simulated (a) SST, (b) moisture transport, and (c) geopotential height and wind at 500 hPa in AM obtained from EXP\_011 - EXP\_CLM. The unit is °C for SST,  $\text{kg m}^{-1} \text{sec}^{-1}$  for moisture transport, m for geopotential height,  $\text{m s}^{-1}$  for wind. Thick black lines in (a) indicate the tropical Pacific region where the model SSTs are prescribed.

CAM3: EXP\_WPW - EXP\_CLM (APR-MAY)

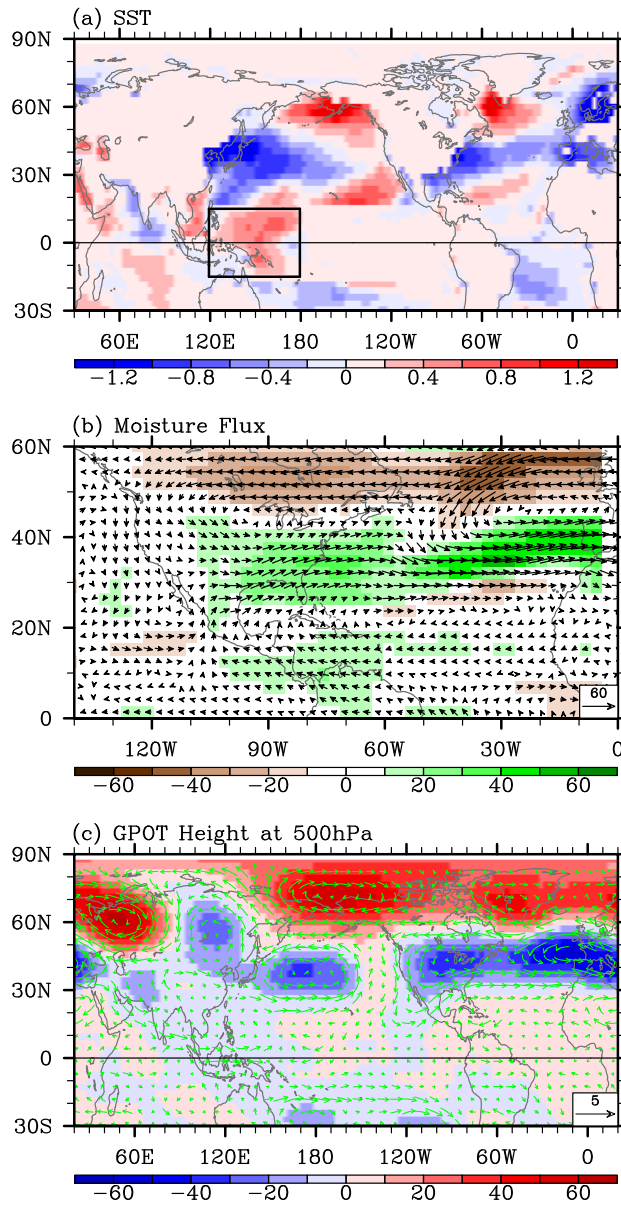


**Figure S8.** Simulated (a) SST, (b) moisture transport, and (c) geopotential height and wind at 500 hPa in AM obtained from EXP\_WPW - EXP\_CLM. The unit is °C for SST, kg m<sup>-1</sup> sec<sup>-1</sup> for moisture transport, m for geopotential height, m s<sup>-1</sup> for wind. Thick black lines in (a) indicate the western Pacific region where the model SSTs are prescribed.



CAM3: Convective Precipitation (APR-MAY)

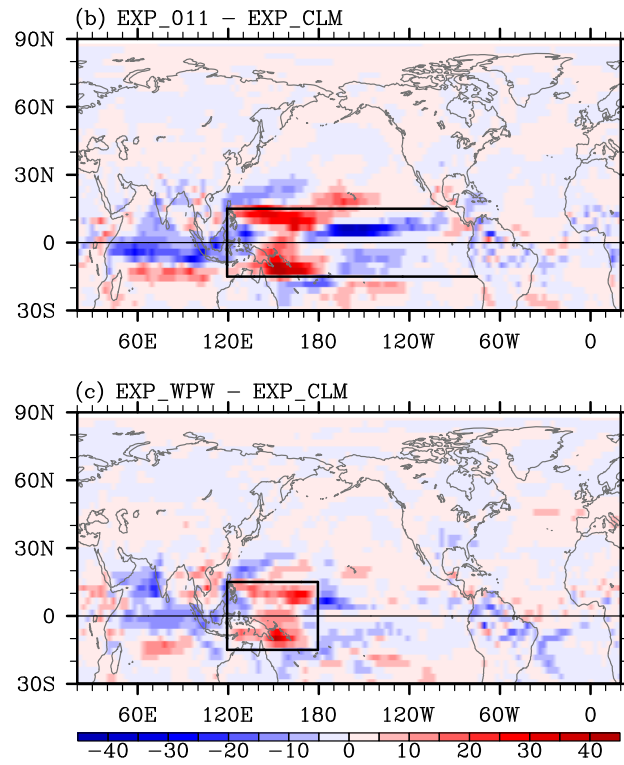


**Figure S9.** Simulated convective precipitation rate in AM obtained from (a) EXP\_011 - EXP\_CLM, and (b) EXP\_WPW - EXP\_CLM. The unit is mm day<sup>-1</sup>.